

## Convective stability of multicomponent fluids in the thermogravitational column

Ilya I. Ryzhkov<sup>1,2,\*</sup> and Valentina M. Shevtsova<sup>1</sup>

<sup>1</sup>MRC, Department of Chemical Physics, Université Libre de Bruxelles, CP 165/62, av. F.D. Roosevelt 50, B-1050 Brussels, Belgium

<sup>2</sup>Institute of Computational Modelling SB RAS, 660036 Krasnoyarsk, Russia

(Received 4 November 2008; published 10 February 2009)

A comprehensive linear stability analysis of convection in the thermogravitational column is first performed for multicomponent fluids. Two types of perturbations are investigated: Longitudinal waves propagating in vertical direction of the column and transversal waves propagating perpendicular to the vertical axis and temperature gradient. The stability problems are reduced to those without cross-diffusion effect by a special transformation. The calculations are performed for binary and ternary mixtures by the Galerkin method. It is found that in binary fluids, the onset of longitudinal instability can be monotonic or oscillatory depending on the separation ratio, which characterizes the Soret effect. The difference between stability characteristics of binary and ternary fluids is associated with different diffusion times of components in a ternary system. It is shown that the mechanism of transversal instability is related to the unstable density stratification in the column (in total or due to individual components). The unstable stratification can only be realized in fluids with negative Soret effect. The analogue of exchange of stabilities principle for a plane column with a multicomponent fluid is proved. The obtained results indicate that the thermogravitational column can be used for measuring diffusion and thermal diffusion coefficients in ternary and higher mixtures with one or several components having negative Soret effect.

DOI: [10.1103/PhysRevE.79.026308](https://doi.org/10.1103/PhysRevE.79.026308)

PACS number(s): 47.20.Bp, 47.57.eb, 66.10.cg

### I. INTRODUCTION

Convection in multicomponent mixtures can show a large variety of dynamical behaviors and flow patterns due to a complex interplay between heat and mass transfer processes. In a multicomponent system, the diffusive mass transport of a given component is induced not only by its concentration gradient, but also by the concentration gradients of the other components (cross diffusion) and the temperature gradient (thermal diffusion or the Soret effect). In binary fluids, the Soret effect can be positive or negative depending on the direction of the lighter component segregation (to the hot or cold region, respectively). The mixtures appearing in nature and industrial applications are essentially multicomponent. Multicomponent convection and relative transport phenomena play an important role in many natural and industrial processes: Oceanic flows, component distribution in hydrocarbon reservoirs, crystal growth, solidification of metallic alloys, etc. [1].

The prediction of heat and mass transfer processes in multicomponent fluids greatly relies on the knowledge of diffusion and thermal diffusion coefficients. Among different methods of their experimental measurement [2–4], the thermogravitational column (TGC) is a well-established technique for binary fluid mixtures. In TGC, the fluid is placed between two vertical walls with different temperatures. The horizontal Soret separation is combined with vertical convective current driven by buoyancy. It leads to an enhanced component separation between the ends of the column. Transient measurements of this separation provide the value of diffusion coefficient, while the thermal diffusion coefficient can be calculated from the steady-state measurements. Ther-

mogravitational column was originally invented by Clusius and Dickel [5]. Furry, Jones, and Onsager [6] developed the column theory for binary mixtures. The impact of compositional dependence of density on the separation process was analyzed in the later works of Nikolaev and Tubin [7] and Navarro *et al.* [8]. Labrosse [9] performed a detailed analysis of steady-state regimes in the column for binary liquid with non-Boussinesq effects (in particular, with variable Soret coefficient). Recently, Haugen and Firoozabadi [10,11] have extended the TGC theory to multicomponent mixtures for steady-state and transient measurements. Ryzhkov and Shevtsova [12] proposed an effective formalism for describing thermal diffusion and convection in systems with many components and applied it to the column theory. In recent years, the first experimental measurements for ternary fluids have been performed by Bou-Ali *et al.* [13] and Leahy-Dios *et al.* [14].

For the successful operation of the column, the stability of vertical convective flow, which drives the separation, is required. The first experimental investigation of stability was performed by Onsager and Watson [15] for a binary gas mixture. Their results were confirmed by a later theoretical work [16] on the basis of linear stability analysis. A recent study [17] provides an extension of this work to binary liquid mixtures. Long-wave instability of multicomponent convection in the column at the initial stage of the separation process was recently investigated by Ryzhkov and Shevtsova [18].

It should be noted that in binary fluids with positive Soret effect, the lighter and heavier components are accumulated at the top and bottom ends of the column, respectively. It provides a gravitationally stable configuration. For negative Soret effect, the situation is opposite and the column is apparently unstable. However, in the experiments with ethanol-water mixtures [19], it was found that the column can be stable when the Soret effect is negative in some range of the applied temperature differences. Linear stability analysis and

\*iryzhkov@ulb.ac.be

full numerical simulations [20] showed that the flow is in fact unstable, but this instability develops very slowly allowing one to observe the separation for some time.

In this paper, we study the stability of stationary convection in the thermogravitational column with a multicomponent fluid. A particular attention is focused on binary and ternary mixtures. The extension of stability analysis to ternary and higher fluids is an important and vital step in the development of the column theory. Presently, the modern methods of experimental measurement (including TGC) are being extended to fluids with more than two components [13,14,21]. It should be noted that in the present study, we pay a particular attention to the stability behavior of fluids with negative Soret effect. The additional motivation of this work is the application of a formalism for describing the influence of thermal diffusion on convection in systems with many components [12].

The paper is organized as follows. Section II describes the basic steady flow and separation in the thermogravitational column. The stability problem is formulated in Sec. III, while the main results for binary, ternary, and multicomponent fluids are presented and discussed in Sec. IV.

## II. STATIONARY CONVECTION IN THE THERMOGRAVITATIONAL COLUMN

Let us first describe the basic steady flow in the column. The stationary solution for this flow was derived in [12] for the general case of a multicomponent system. Here we only present the problem statement and provide the final formulas to be used in the stability calculations.

Consider a mixture with  $n$  components, where component  $n$  is chosen as a solvent and the composition is given by  $\mathbf{C} = (C_1, \dots, C_{n-1})^T$  (the superscript denotes a column vector). It is assumed that the density is a linear function of temperature and composition,

$$\begin{aligned} \rho &= \rho_0 \left( 1 - \beta_T(T - T_0) - \sum_{i=1}^{n-1} \beta_i(C_i - C_{i0}) \right) \\ &= \rho_0 [1 - \beta_T(T - T_0) - \mathbf{I} \cdot \mathbf{B} \cdot (\mathbf{C} - \mathbf{C}_0)]. \end{aligned} \quad (1)$$

Here  $\rho_0$  is the mean fluid density,  $\beta_T$  and  $\beta_i$  are the thermal and solutal expansion coefficients, respectively,  $\mathbf{B} = \text{diag}\{\beta_1, \dots, \beta_{n-1}\}$  is the diagonal matrix, and  $\mathbf{I} = (1, \dots, 1)$  is  $(n-1)$ -dimensional vector. The equations of multicomponent convection in the Boussinesq approximation have the form

$$\begin{aligned} \partial_t \mathbf{U} + (\mathbf{U} \cdot \nabla) \mathbf{U} &= -\rho_0^{-1} \nabla P + \nu \nabla^2 \mathbf{U} - \mathbf{g} [\beta_T(T - T_0) \\ &\quad + \mathbf{I} \cdot \mathbf{B} \cdot (\mathbf{C} - \mathbf{C}_0)], \\ \partial_t T + (\mathbf{U} \cdot \nabla) T &= \chi \nabla^2 T, \\ \partial_t \mathbf{C} + (\mathbf{U} \cdot \nabla) \mathbf{C} &= D \nabla^2 \mathbf{C} + \mathbf{D}_T \nabla^2 T, \\ \nabla \cdot \mathbf{U} &= 0. \end{aligned} \quad (2)$$

Here  $\mathbf{U}$  is the velocity vector,  $P$  is the pressure,  $\nu$  is the kinematic viscosity,  $\chi$  is the thermal diffusivity,  $D$  is

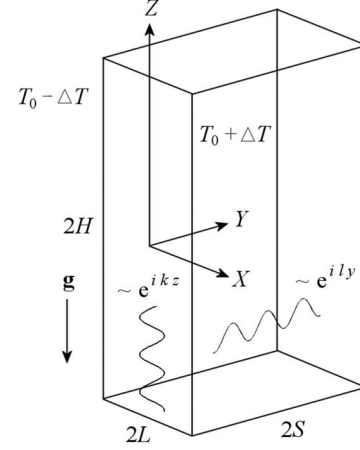


FIG. 1. Geometry of the column.

the matrix of  $(n-1)^2$  diffusion coefficients,  $\mathbf{D}_T = (D_{T1}, \dots, D_{Tn-1})^T$  is the vector of thermal diffusion coefficients, and  $\mathbf{g} = (0, 0, -g)$  is the gravitational acceleration.

Let us consider a plane thermogravitational column of height  $2H$ , thickness  $2L$ , and transversal width  $2S$  (Fig. 1). The lateral walls  $X = \pm L$  are maintained at constant but different temperatures  $T_0 \pm \Delta T$ . It is supposed that there is no vertical temperature gradient. In the column, the horizontal temperature gradient induces horizontal gradients of composition due to the Soret effect and also results in convective flow driven by buoyancy force. The aspect ratios of the column are  $H/L \sim 10^2$  and  $S/L \sim 10$ , so the flow can be assumed to be two dimensional (in  $XZ$  plane) and strictly vertical (except at the top and bottom ends of the slot). Zero horizontal velocity and continuity imply that the vertical velocity component varies in the horizontal direction only. The horizontal separation of components combined with vertical convective currents leads to an enhanced separation between the top and bottom ends. In the steady-state regime, the vertical concentration gradients are assumed to be constant.

According to this configuration, the basic steady state is sought in the form

$$\mathbf{U} = (0, 0, W(X)), \quad T = T_0 + T(X), \quad \mathbf{C} = \mathbf{C}_0 + \mathbf{C}(X) + \mathbf{A}Z, \quad (3)$$

where  $\mathbf{A} = (A_1, \dots, A_{n-1})^T$  is a constant vector. Let us introduce the dimensionless coordinate vector  $\mathbf{x}$ , velocity  $\mathbf{u}$ , pressure  $p$ , temperature  $\Theta$ , and concentrations  $\mathbf{c} = (c_1, \dots, c_{n-1})^T$  by the formulas

$$\begin{aligned} \mathbf{X} = L\mathbf{x}, \quad \mathbf{U} &= \frac{g\beta_T\Delta TL^2}{\nu} \mathbf{u}, \quad P = \rho_0 g L \beta_T \Delta T p, \\ T - T_0 &= \Delta T \Theta, \quad \mathbf{C} - \mathbf{C}_0 = \beta_T \Delta T \mathbf{B}^{-1} \mathbf{c}. \end{aligned} \quad (4)$$

Taking the time scale as  $L^2/\nu$ , we can rewrite equations (2) in dimensionless form

$$\begin{aligned} \partial_t \mathbf{u} + \text{Gr}(\mathbf{u} \cdot \nabla) \mathbf{u} &= -\nabla p + \nabla^2 \mathbf{u} + (\Theta + \mathbf{I} \cdot \mathbf{c}) \mathbf{e}, \\ \partial_t \Theta + \text{Gr}(\mathbf{u} \cdot \nabla) \Theta &= \text{Pr}^{-1} \nabla^2 \Theta, \end{aligned}$$

$$\begin{aligned} \partial_t \mathbf{c} + \text{Gr}(\mathbf{u} \cdot \nabla) \mathbf{c} &= \mathcal{S}(\nabla^2 \mathbf{c} - \boldsymbol{\psi} \nabla^2 \Theta), \\ \nabla \cdot \mathbf{u} &= 0, \end{aligned} \quad (5)$$

where  $\mathbf{e} = (0, 0, 1)$ . The system includes the Grashof number  $\text{Gr} = g\beta_T \Delta T L^3 / \nu^2$ , the Prandtl number  $\text{Pr} = \nu / \chi$ , and the square matrix of  $(n-1)^2$  dimensionless parameters

$$S = \nu^{-1} B D B^{-1}, \quad \{S\}_{ij} = \frac{\beta_i}{\beta_j} \frac{1}{\text{Sc}_{ij}}, \quad i, j = 1, \dots, n-1,$$

where  $\text{Sc}_{ij} = \nu / D_{ij}$  are the Schmidt numbers. The dimensionless separation ratios

$$\boldsymbol{\psi} = (\psi_1, \dots, \psi_{n-1})^T = -\beta_T^{-1} B D^{-1} \mathbf{D}_T$$

characterize the separation of components due to the Soret effect. Suppose that the thermal expansion is normal ( $\beta_T > 0$ ), which is the case for most fluids. Then it can be shown that in the case of positive  $\psi_i$ , component  $i$  is driven by thermal diffusion to the hot or cold region depending on whether it is lighter ( $\beta_i > 0$ ) or heavier ( $\beta_i < 0$ ) than the solvent, respectively. If  $\psi_i$  is negative, then the lighter (heavier) component  $i$  is driven to the cold (hot) region. Depending on the sign of  $\psi_i$ , we will speak about positive or negative Soret effect of a particular component.

To characterize a multicomponent system as a whole with respect to the Soret effect, the net separation ratio is introduced by the formula

$$\Psi = \sum_{i=1}^{n-1} \psi_i. \quad (6)$$

It can be shown that this parameter does not depend on the choice of solvent (while the values of  $\psi_i$  depend on this choice) and is uniquely defined for a given multicomponent system. A detailed description of separation ratios and their properties can be found in [12], where these parameters were first introduced for multicomponent fluids.

The flow in the thermogravitational column should satisfy a number of conditions. On the lateral walls, the no-slip condition, the temperature difference, and the absence of diffusive fluxes are imposed:

$$x = \pm 1, \quad \mathbf{u} = 0, \quad \Theta = \pm 1, \quad \frac{\partial \mathbf{c}}{\partial x} - \boldsymbol{\psi} \frac{\partial \Theta}{\partial x} = 0. \quad (7)$$

In dimensionless variables, the general form of the basic state (3) is written as

$$\mathbf{u} = (0, 0, w(x)), \quad \Theta = \Theta(x), \quad \mathbf{c} = \mathbf{c}(x) + \text{Gr}^{-1} \mathcal{S} \mathcal{R}_z, \quad (8)$$

where

$$\mathcal{R} = (R_1, \dots, R_{n-1})^T = \frac{gL^4}{\nu} B D^{-1} \mathbf{A}$$

is the vector of solutal Rayleigh numbers defined through the vertical concentration gradients

The sum

$$R = R_1 + \dots + R_{n-1}$$

is termed the net solutal Rayleigh number.

The additional conditions on the basic state are zero flow rate through any horizontal cross section and conservation of mass for each component,

$$\int_{-1}^1 w dx = 0, \quad \int_{-1}^1 c dx = 0. \quad (9)$$

The net vertical flux through any cross section should also be zero (see [12] for further details),

$$\int_{-1}^1 c u dx - \frac{2}{\text{Gr}^2} \mathcal{S}^2 \mathcal{R} = 0. \quad (10)$$

The second term in this equation represents the contribution of diffusion in vertical direction of the column. It can be neglected when the Grashof number is large enough and diffusive properties of the medium are weak. Let us first provide the solution of the problem when the vertical diffusion is negligible (the opposite case will be considered later). The representation of solution depends on the net separation ratio  $\Psi$  defined by (6).

#### A. Case $\Psi > 0$

The velocity, temperature and composition are given by

$$w_s = \frac{\Psi + 1}{\eta^3} \frac{\sin \eta \cosh \eta \sinh \eta x \cos \eta x - \sinh \eta \cos \eta \sin \eta x \cosh \eta x}{\sin 2\eta + \sinh 2\eta}, \quad \Theta_s = x,$$

$$\mathbf{c}_s = \left[ (1 + \Psi^{-1}) \left( \frac{2 \sin \eta \cosh \eta \sin \eta x \cosh \eta x + 2 \sinh \eta \cos \eta \sinh \eta x \cos \eta x}{\eta(\sin 2\eta + \sinh 2\eta)} - x \right) + x \right] \boldsymbol{\psi} + \frac{1}{\text{Gr}} \mathcal{S} \mathcal{R}_z,$$

where  $\eta = (R/4)^{1/4}$ . The subscript  $s$  indicates the stationary state. The net solutal Rayleigh number  $R > 0$  is related to the net separation ratio by the equation

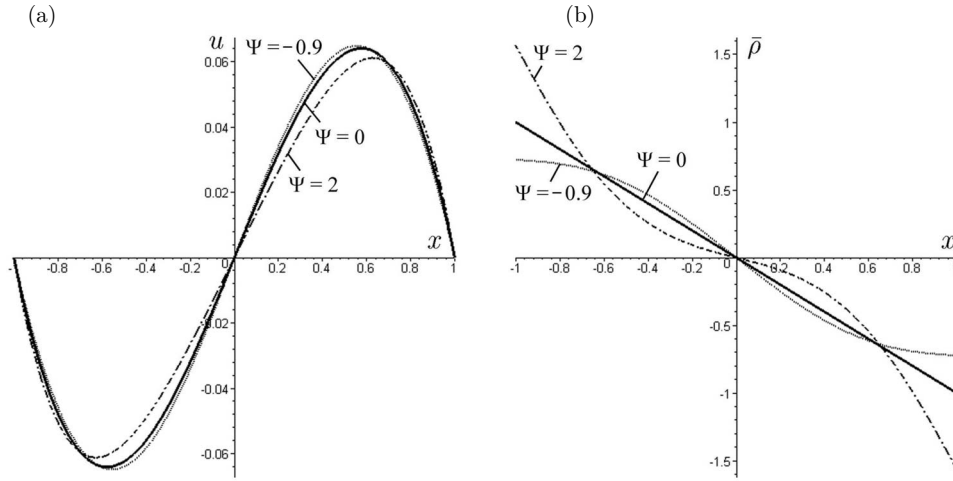


FIG. 2. The profiles of dimensionless velocity and density for different values of the net separation ratio  $\Psi$ .

$$\Psi = \frac{G(\eta)}{F(\eta) - G(\eta)}, \quad \eta = (R/4)^{1/4}, \quad (11)$$

where

$$F(\eta) = 1 + \frac{1 \cos 2\eta - \cosh 2\eta}{\eta \sin 2\eta + \sinh 2\eta},$$

$$G(\eta) = 1 + \frac{5 \cos 2\eta - \cosh 2\eta}{4\eta \sin 2\eta + \sinh 2\eta} + \frac{\sin 2\eta \sinh 2\eta}{(\sin 2\eta + \sinh 2\eta)^2}. \quad (12)$$

Equation (11) has a unique solution. The solutal Rayleigh numbers are found from

$$\mathcal{R} = \frac{R}{\Psi} \psi. \quad (13)$$

### B. Case $\Psi < 0$ , $\Psi \neq -1$

In this case, the solution has the form

$$w_s = \frac{\Psi + 1 \sinh \gamma \sin \gamma x - \sin \gamma \sinh \gamma x}{\gamma^3 \sin \gamma \cosh \gamma + \sinh \gamma \cos \gamma}, \quad \Theta_s = x,$$

$$c_s = \left[ (1 + \Psi^{-1}) \left( \frac{\sin \gamma \sinh \gamma x + \sinh \gamma \sin \gamma x}{\gamma(\sin \gamma \cosh \gamma + \sinh \gamma \cos \gamma)} - x \right) + x \right] \psi + \frac{1}{\text{Gr}} \mathcal{S} \mathcal{R} z,$$

where  $\gamma = (-R)^{1/4}$ . The net solutal Rayleigh number  $R < 0$  is related to  $\Psi$  by the equation

$$\Psi = \frac{G(\gamma)}{F(\gamma) - G(\gamma)}, \quad \gamma = (-R)^{1/4}, \quad (14)$$

where

$$F(\gamma) = 1 - \frac{2 \sin \gamma \sinh \gamma}{\gamma(\sin \gamma \cosh \gamma + \sinh \gamma \cos \gamma)},$$

$$G(\gamma) = 1 - \frac{5 \sin \gamma \sinh \gamma}{2\gamma(\sin \gamma \cosh \gamma + \sinh \gamma \cos \gamma)} + \frac{\sin^2 \gamma + \sinh^2 \gamma}{2(\sin \gamma \cosh \gamma + \sinh \gamma \cos \gamma)^2}. \quad (15)$$

The solution of Eq. (14) is unique for  $\Psi > -1$  and nonunique when  $\Psi < -1$ . The solutal Rayleigh numbers are determined from (13).

### C. Case $\Psi = 0$

Here we also have  $R=0$  and the solution is given by

$$w_s = \frac{x - x^3}{6}, \quad \Theta_s = x,$$

$$c_s = -\frac{21x^5 - 70x^3 + 25x}{80} \psi + \frac{1}{\text{Gr}} \mathcal{S} \mathcal{R} z, \quad \mathcal{R} = \frac{63}{2} \psi.$$

### D. Case $\Psi = -1$

In this case, the solution is written as

$$w_s = 0, \quad \Theta_s = x, \quad c_s = \psi x, \quad \mathcal{R} = 0.$$

There is no convective flow since the contributions of temperature and composition to the density profile in the cross section compensate each other.

*Statement 1.* The sign of net solutal Rayleigh number  $R$  always coincides with the sign of net separation ratio  $\Psi$  [12]. The corresponding parameters of individual components,  $R_i$  and  $\psi_i$ , also have the same signs [it follows from (13)].

To analyze the effect of thermal diffusion on convection in the basic state, we introduce the dimensionless density variation by using (1) and (4),

$$\bar{\rho} = (\rho - \rho_0) / \rho_0 \beta_T \Delta T = -\Theta - \mathbf{I} \cdot \mathbf{c}. \quad (16)$$

In what follows, the partial dimensionless densities  $\rho_i = -c_i$ ,  $i=1, \dots, n-1$  will also be used. The profiles of dimensionless velocity and density at  $z=0$  are presented in Fig. 2 for

different values of the net separation ratio. When  $\Psi=0$ , the net effect of concentration variations on the fluid density is zero and thermal expansion results in the linear density profile, which drives convective motion. For positive  $\Psi$ , the density variations are decreased in the center of the column and increased at the walls. As a result, convective motion develops closer to the boundaries. In this case, the net effect of thermal diffusion is to bring the lighter and heavier components to the hot and cold walls, respectively (provided that  $\beta_T > 0$ ). Due to convective current, the lighter (heavier) species are accumulated at the Top (bottom) part of the column. It provides a potentially stable vertical stratification. When  $\Psi$  is negative, the lighter (heavier) components segregate to the cold (hot) wall. Here the vertical stratification is potentially unstable since convection drives the lighter (heavier) species to the bottom (top) part of the column.

### E. Role of vertical diffusion

When vertical diffusion is taken into account [the second term in Eq. (10)], formulas (11), (13), and (14) are no longer valid. The solutal Rayleigh numbers are found from the non-linear system of equations

$$\mathcal{R} = \frac{R}{\Psi + 1} \frac{F}{G} \left( E + \frac{R^2}{\text{Gr}^2 (\Psi + 1)^2 G} \mathcal{S}^2 \right)^{-1} \boldsymbol{\psi}, \quad (17)$$

where  $E$  is the unity matrix. The functions  $F$  and  $G$  are given by (12) and (15) for positive and negative  $\Psi$ , respectively. It was shown in [12] that for  $-1 < \Psi < 2$ , the vertical diffusion can be neglected when

$$\begin{aligned} \text{Gr Sc}_M > 3765, \quad \text{where } \text{Sc}_M \\ = \left( \max_{i,j} \left| \frac{\beta_i}{\beta_j} \sum_{k=1}^{n-1} \frac{1}{\text{Sc}_{ik} \text{Sc}_{kj}} \right| \right)^{-1/2}. \end{aligned} \quad (18)$$

As an example, let us consider a ternary mixture with  $\psi_1 = -0.1$ ,  $\psi_2 = 0.4$ ,  $\text{Sc}_{11} = 100$ ,  $\text{Sc}_{22} = 500$ ,  $\text{Sc}_{12} = \text{Sc}_{21} = \infty$  (i.e., cross diffusion is neglected). In this case, criteria (18) provides  $\text{Gr} > 37.65$ . Figure 3 presents the dependence of two solutal Rayleigh numbers on the Grashof number. One can see that vertical diffusion is important only for small Grashof numbers, i.e., when convection in vertical direction is weak. In real TGC experiments, the spacing of the column  $L$  is chosen in such a way that vertical convection is rather strong and vertical separation does not depend on  $\Delta T$  [22].

### III. STABILITY PROBLEM

To investigate the stability of the basic flow, we represent the velocity, pressure, temperature, and concentration fields as a sum of the basic state  $w_s, \Theta_s, \mathbf{c}_s$  and small perturbations. Equations (5) are linearized around the basic state. It should be noted that in the present configuration, the Squire's transformation [23] is not valid, so the most unstable disturbances can be, in general, three dimensional.

In this work, we investigate two types of normal perturbations (see Fig. 1) Longitudinal waves  $\mathbf{u} = (-\Phi_z, 0, \Phi_x)$ ,  $\Theta$ ,  $\mathbf{c}$ , in  $XZ$  plane, which have the form

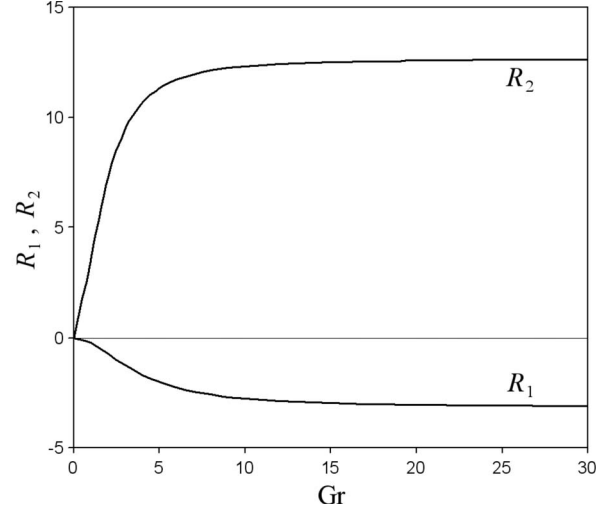


FIG. 3. The dependence of solutal Rayleigh numbers on the Grashof number for ternary fluid with  $\psi_1 = -0.1$ ,  $\psi_2 = 0.4$ ,  $\text{Sc}_{11} = 100$ ,  $\text{Sc}_{22} = 500$ .

$$(\Phi, \Theta, \mathbf{c}) = (\varphi(x), \theta(x), \boldsymbol{\xi}(x)) \exp(-\lambda t + ikz), \quad (19)$$

where  $\Phi$  is the stream function, and transversal waves  $\mathbf{u} = (0, v, w)$ ,  $\Theta$ ,  $\mathbf{c}$  in  $YZ$  plane given by

$$(v, w, \Theta, \mathbf{c}) = (v(x), w(x), \theta(x), \boldsymbol{\xi}(x)) \exp(-\mu t + i ly). \quad (20)$$

In what follows, the complex growth rates will be written as  $\lambda = \lambda_r + i\lambda_\omega$  and  $\mu = \mu_r + i\mu_\omega$ .

### A. Longitudinal waves

For this type of perturbations [Eq. (19)], we use two-dimensional equations (5) in the stream function formulation. It is convenient to introduce a new variable  $\boldsymbol{\eta} = \boldsymbol{\xi} - \boldsymbol{\psi}\theta$ . The stability problem is written in the form

$$\Delta^2 \varphi + ik \text{Gr} (w_s'' \varphi - w_s \Delta \varphi) + (1 + \Psi) \theta' + \mathbf{I} \cdot \boldsymbol{\eta}' = -\lambda \Delta \varphi, \quad (21)$$

$$\text{Pr}^{-1} \Delta \theta + ik \text{Gr} (\Theta_s' \varphi - w_s \theta) = -\lambda \theta, \quad (22)$$

$$S(\Delta \boldsymbol{\eta} - \mathcal{R} \varphi') + ik \text{Gr} [\mathbf{c}_s' \varphi - w_s (\boldsymbol{\eta} + \boldsymbol{\psi}\theta)] = -\lambda (\boldsymbol{\eta} + \boldsymbol{\psi}\theta). \quad (23)$$

Here  $\Delta = \partial_{xx} - k^2$  and the prime stands for  $\partial_x$ . The boundary conditions follow from (7):

$$x = \pm 1, \quad \varphi = \varphi' = 0, \quad \theta = 0, \quad \boldsymbol{\eta}' = 0. \quad (24)$$

The stability equations are solved by the Galerkin method. The solution is sought in the form of expansions

$$\varphi = \sum_{j=0}^J a_j \varphi_j, \quad \theta = \sum_{m=0}^M b_m \theta_m, \quad \boldsymbol{\eta} = \sum_{q=0}^Q \sum_{i=1}^{n-1} c_{qi} \boldsymbol{\eta}_{qi},$$

where the basic functions are the eigenfunctions of the following problems:



$$\Delta^2 \varphi_j = -\lambda_j \Delta \varphi_j, \quad x = \pm 1, \quad \varphi_j = \varphi_j' = 0, \quad (25)$$

$$\text{Pr}^{-1} \Delta \theta_m = -\mu_m \theta_m, \quad x = \pm 1, \quad \theta_m = 0, \quad (26)$$

$$S \Delta \boldsymbol{\eta}_{qi} = -\nu_{qi} \boldsymbol{\eta}_{qi}, \quad x = \pm 1, \quad \boldsymbol{\eta}_{qi}' = 0. \quad (27)$$

Problems (25)–(27) are derived from the corresponding equations (21)–(23) with boundary conditions (24). The present choice of basic functions is based on considering the disturbances of stream function, temperature, and composition in an isothermal fluid layer ( $\text{Gr}=0$ ) independently of each other. The basis used in this work is an extension of the basis for a single-component fluid [24] to multicomponent mixtures.

Problem (25) has even and odd solutions. The even eigenfunctions are

$$\varphi_j = \frac{1}{\sqrt{I_j}} \left( \frac{\cosh kx}{\cosh k} - \frac{\cos \sqrt{\lambda_j - k^2} x}{\cos \sqrt{\lambda_j - k^2}} \right), \quad j = 0, 2, 4, \dots,$$

$$I_j = \frac{\lambda_j}{k^2 - \lambda_j} (k^2 + k \tanh k - k^2 \tanh^2 k - \lambda_j),$$

where the eigenvalues  $\lambda_j$  are the roots of the equation  $\sqrt{\lambda_j - k^2} \tan \sqrt{\lambda_j - k^2} + k \tanh k = 0$ . The odd eigenfunctions have the form

$$\varphi_j = \frac{1}{\sqrt{I_j}} \left( \frac{\sinh kx}{\sinh k} - \frac{\sin \sqrt{\lambda_j - k^2} x}{\sin \sqrt{\lambda_j - k^2}} \right), \quad j = 1, 3, 5, \dots,$$

$$I_j = \frac{\lambda_j}{k^2 - \lambda_j} (k^2 + k \coth k - k^2 \coth^2 k - \lambda_j),$$

while the corresponding eigenvalues satisfy the equation  $\sqrt{\lambda_j - k^2} \cot \sqrt{\lambda_j - k^2} + k \coth k = 0$ .

Problem (26) has the following solutions:

$$\mu_m = \text{Pr}^{-1} [\pi^2/4(m+1)^2 + k^2],$$

$$\theta_m = \begin{cases} \cos[\pi/2(m+1)x], & m = 0, 2, 4, \dots, \\ \sin[\pi/2(m+1)x], & m = 1, 3, 5, \dots \end{cases} \quad (28)$$

For a mixture with  $n$  components, system (27) has  $n-1$  series of eigenfunctions and eigenvalues,

$$\nu_{qi} = \nu_i (\pi^2 q^2/4 + k^2),$$

$$\boldsymbol{\eta}_{qi} = \boldsymbol{\eta}_i \begin{cases} \sqrt{2}/2, & q = 0, \\ \sin(\pi/2qx), & q = 1, 3, 5, \dots, \\ \cos(\pi/2qx), & q = 2, 4, 6, \dots, \end{cases} \quad (29)$$

where  $\nu_i$  and  $\boldsymbol{\eta}_i$  are the eigenvalues and the corresponding eigenvectors of the matrix  $S$ ,  $i = 1, \dots, n-1$ .

In the numerical calculations, the number of basic functions was taken as  $J=M=15$ ,  $Q=20$  for determining the structure of neutral curves on the plane ( $k$ ,  $\text{Gr}$ ), and  $J=M=25$ ,  $Q=30$  for minimizing these curves over  $k$ . So, the total number of functions  $J+M+(n-1)Q$  was 50–70 for binary fluids and 70–100 for ternary fluids.

## B. Transversal waves

Substituting representation (20) into the three-dimensional linearized equations, we find  $v=0$ . The stability problem reduces to

$$\Delta w + \theta + \mathbf{I} \cdot \boldsymbol{\xi} = -\mu w, \quad (30)$$

$$\text{Pr}^{-1} \Delta \theta = -\mu \theta, \quad (31)$$

$$S(\Delta \boldsymbol{\xi} - \boldsymbol{\psi} \Delta \theta - \mathcal{R} w) = -\mu \boldsymbol{\xi}, \quad (32)$$

$$x = \pm 1, \quad w = 0, \quad \theta = 0, \quad \boldsymbol{\xi}' - \boldsymbol{\psi} \theta' = 0, \quad (33)$$

where  $\Delta = \partial_{xx} - l^2$ . Equation (31) together with the boundary condition  $\theta=0$  at  $x = \pm 1$  can be solved separately from the other equations. Its eigenvalues and eigenfunctions are given by (28). Since all eigenvalues  $\mu_m$  are positive, the transversal temperature perturbations and the corresponding perturbations of velocity and composition decay monotonically. The latter are obtained by setting  $\mu = \mu_m$ ,  $\theta = \theta_m$  and solving Eqs. (30) and (32) subject to boundary conditions (33). So, non-decaying transversal perturbations are possible only when  $\theta = 0$ . In this case, the stability problem reduces to

$$\Delta w + \mathbf{I} \cdot \boldsymbol{\xi} = -\mu w, \quad (34)$$

$$S(\Delta \boldsymbol{\xi} - \mathcal{R} w) = -\mu \boldsymbol{\xi}, \quad (35)$$

$$x = \pm 1, \quad w = 0, \quad \boldsymbol{\xi}' = 0. \quad (36)$$

Here the solutal Rayleigh numbers  $\mathcal{R} = \mathcal{R}(\boldsymbol{\psi}, S, \text{Gr})$  are found from (17) and depend on the physical properties of the fluid and the Grashof number.

The stability problem is solved by the Galerkin method. The solution is represented in the form of expansions

$$w = \sum_{m=0}^M b_m w_m, \quad \boldsymbol{\xi} = \sum_{q=0}^Q \sum_{i=1}^{n-1} c_{qi} \boldsymbol{\xi}_{qi}. \quad (37)$$

The basic functions are given by (28) and (29), where one should replace  $\theta$  and  $\boldsymbol{\eta}$  by  $w$  and  $\boldsymbol{\xi}$ , respectively. The analysis showed that the number of basic functions  $M=Q=20$  is sufficient for accurate determination of neutral curves.

## C. On the cross-diffusion effect

The described stability problem contains a large number of control parameters. In particular, the dimensionless diffusion matrix  $S$  is formed by  $(n-1)^2$  Schmidt numbers for a mixture with  $n$  components. To reduce the number of control parameters in problems of multicomponent convection with the Soret effect, a special transformation of composition and separation ratios was suggested in [25],

$$\mathbf{c} = P Q^{-1} \mathbf{c}, \quad \boldsymbol{\psi} = P Q^{-1} \boldsymbol{\psi}'. \quad (38)$$

Here  $P$  is the matrix, which columns are formed by the eigenvectors  $\boldsymbol{\eta}_i$  of the matrix  $S$ ,  $i = 1, \dots, n-1$ , and

$$Q = \text{diag}\{\mathbf{I} \cdot \boldsymbol{\eta}_1, \dots, \mathbf{I} \cdot \boldsymbol{\eta}_{n-1}\}$$

is a diagonal matrix, where  $\mathbf{I} = (1, \dots, 1)$  is  $(n-1)$ -dimensional vector. Transformation (38) reduces governing

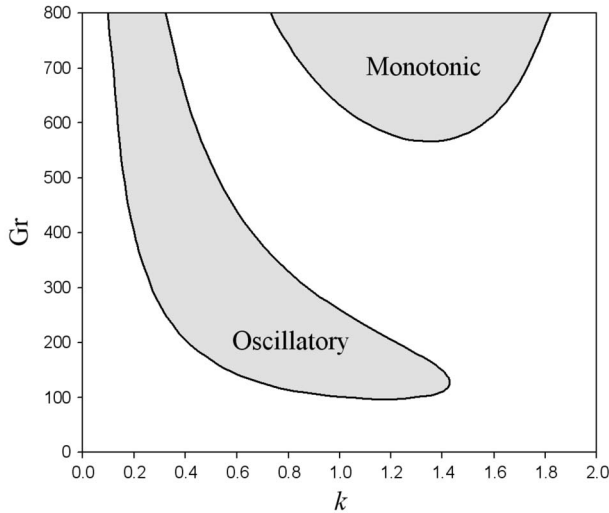


FIG. 4. Neutral curves for longitudinal perturbations in a binary fluid with  $\Psi=0.5$ ,  $Sc=500$ .

equations (5) as well as imposed conditions (7), (9), and (10) to those with a diagonal matrix  $S' = P^{-1}SP$ , separation ratios  $\psi'$ , and composition  $c'$ . It can be easily checked that the same is true for the stability problems (21)–(24) and (34)–(36). So, one can say that in the present configuration, the original multicomponent system is equivalent to another system without cross diffusion but with different separation ratios and composition.

*Statement 2.* The net separation ratio  $\Psi = \psi_1 + \dots + \psi_{n-1}$  and the sum of dimensionless concentrations  $c_1 + \dots + c_{n-1}$  are invariant under transformation (38) [25].

In the stability calculations below, we assume that the matrix  $S$  is diagonal [or transformed to this form by (38)].

## IV. RESULTS AND DISCUSSION

### A. Instability in binary fluids

Let us start with the stability results for binary systems. These results are required for understanding a more complicated behavior of ternary fluids. The calculations for binary mixtures presented below provide the extension of the previous findings [16,17,20] to a wider range of control parameters. In this work, we focus our attention on liquids and fix the Prandtl number at  $Pr=10$ .

Figure 4 presents a typical structure of neutral curves for longitudinal perturbations in a binary fluid with  $\Psi=0.5$ ,  $Sc=500$ . Here we have two instability modes, monotonic and oscillatory. In the presented case, the latter is a more dangerous one. The calculations show that with decreasing the separation ratio  $\Psi$ , the oscillatory curve is shifted upwards and monotonic mode becomes more dangerous. It should be noted that the structure of neutral curves for ternary fluids is similar to that of Fig. 4.

The dependence of critical Grashof number, wave numbers  $k$ ,  $l$ , and frequency on the separation ratio  $\Psi$  is presented in Fig. 5. We consider the range  $\Psi > -1$  only since the basic state is nonunique for  $\Psi < -1$  (see Sec. II B). The solid lines correspond to longitudinal perturbations. Calculations

show that the monotonic mode remains almost unchanged with the variation of Prandtl and Schmidt numbers, so this type of instability does not depend on the thermal and diffusive properties of the fluid. The analysis of perturbation structure reveals that the instability develops in the form of vortices on the boarder line between two counterflows, see Figs. 2 and 8 (the latter refers to ternary fluids, where the structure of perturbations is similar to binary case). The increase of the separation ratio  $\Psi$  has a stabilizing effect on the monotonic mode. Note that for positive  $\Psi$ , the lighter (heavier) component accumulates at top (bottom) part of the column providing a potentially stable vertical stratification. When  $\Psi$  is increased, this stratification becomes stronger and stabilizes the monotonic mode. For negative  $\Psi$ , the vertical stratification is potentially unstable, so the monotonic stability boundary is decreasing. With increasing the separation ratio, the oscillatory mode becomes more dangerous and leads to a strong destabilization of the flow. This mode essentially depends on the diffusive properties of the medium: Strong diffusion (i.e., small Schmidt number) favors the decay of compositional perturbations and stabilizes the flow. However, for large Schmidt numbers, diffusion is rather weak and the flow is less stable. The calculations show that the oscillatory instability is associated with the growth of two perturbations with opposite phase velocities  $\lambda_\omega/k$ . It should be noted that for both monotonic and oscillatory modes, the critical wave number decreases with increasing the critical Grashof number.

The dashed lines in Fig. 5 correspond to the transversal perturbations. We found that for negative separation ratios, the flow is unstable at any value of the Grashof number with the critical wave number  $l=0$ . The long-wave instability is caused by the accumulation of the heavier component at the top part of the column (in this case, the vertical density gradient is gravitationally unstable). This instability mechanism is expected for negative  $\Psi$ , but cannot be revealed by considering only two-dimensional perturbations in  $XZ$  plane.

It should be noted that in this paper, we use Boussinesq approximation and assume that the density is a linear function of temperature and composition. The influence of non-Boussinesq effects, and, in particular, the impact of variable separation ratio  $\Psi(T, C)$  on the steady-state regimes in the column with binary fluid were investigated in [9]. Despite a more complex dependence of the system behavior on the control parameters, two categories of steady flows were distinguished, according to whether the vertical stratification is potentially stable or unstable. Thus, one can expect that the general stability characteristics discussed in this section are relevant to non-Boussinesq fluids also.

### B. Ternary fluids: Longitudinal perturbations

In this section, we proceed to the stability of ternary fluids in the thermogravitational column. The following assumptions can be made without loss of generality.

(1) The heaviest component is chosen as a solvent, so the solutal expansion coefficients  $\beta_i$  are positive. In addition, we assume that the thermal expansion  $\beta_T > 0$  (the case of negative  $\beta_T$  can be treated similarly). Under these assumptions,

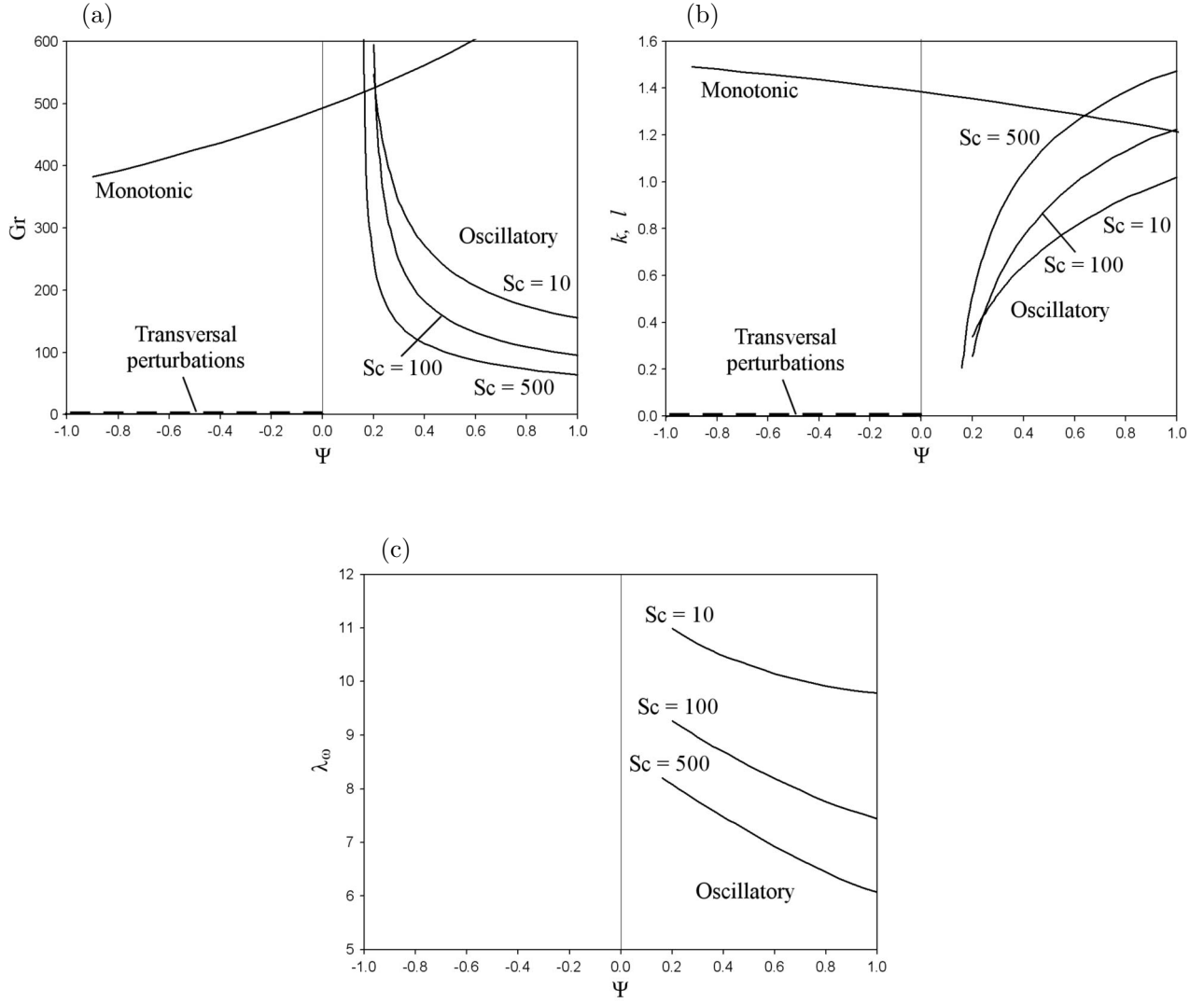


FIG. 5. The dependence of critical Grashof number (a), wave numbers (b), and frequency (c) on the separation ratio  $\Psi$  for binary fluid. Solid and dashed lines correspond to longitudinal and transversal perturbations, respectively.

component  $i$  is driven to the hot (cold) region when the separation ratio  $\psi_i$  is positive (negative),  $i=1,2$ .

(2) The dimensionless diffusion matrix is assumed to be diagonal:  $\mathcal{S} = \text{diag}\{Sc_{11}, Sc_{22}\}$  [otherwise, it can be diagonalized by transformation (38)]. In addition, we suppose that the ratio  $s = Sc_{11}/Sc_{22}$  satisfies the inequality  $0 < s \leq 1$  (otherwise, one can change the numbering of components). This parameter can be also written as the ratio of diffusion times of components:  $s = \tau_1/\tau_2$ , where  $\tau_i = L^2/D_{ii}$ .

In what follows, a ternary fluid will be characterized by the parameters  $\Psi$ ,  $\psi_1$ ,  $s$ ,  $Sc_{22}$ . It should be noted that if the dependence of some characteristic (e.g., critical Grashof number) on these parameters is known, one can easily account for the cross-diffusion effect by making the change according to (38),

$$s \rightarrow \frac{\nu_2}{\nu_1}, \quad Sc_{22} \rightarrow \frac{1}{\nu_2},$$

$$\psi_1 \rightarrow \frac{\nu_1 + \delta Sc_{12}^{-1} - Sc_{11}^{-1}}{\nu_2 - \nu_1} \left[ \left( \frac{Sc_{12}(\nu_2 - Sc_{11}^{-1})}{\delta} + 1 \right) \psi_1 - \Psi \right],$$

where

$$\nu_{1,2} = \frac{1}{2} [Sc_{11}^{-1} + Sc_{22}^{-1} \pm \sqrt{(Sc_{11}^{-1} - Sc_{22}^{-1})^2 + 4 Sc_{12}^{-1} Sc_{21}^{-1}}]$$

are the eigenvalues of matrix  $\mathcal{S}$  and  $\delta = \beta_1/\beta_2$ .

Let us first consider a ternary mixture with the same diffusive properties of two components, i.e.,  $s=1$ . Calculations show that the stability diagram for such mixture coincides with that for binary fluid (see Fig. 5), where  $\Psi = \psi_1 + \psi_2$  is now the net separation ratio. The important fact is that the stability boundaries do not depend on the individual values of  $\psi_1$  and  $\psi_2$ . When the ratio of Schmidt numbers (or diffusion times)  $s \neq 1$ , ternary effects come into play. However, the monotonic mode is still determined by the value of net separation ratio  $\Psi$  only. A typical structure of critical perturbations for monotonic instability is shown in Fig. 8. One can clearly see the pairs of counter-rotating vortices, which de-



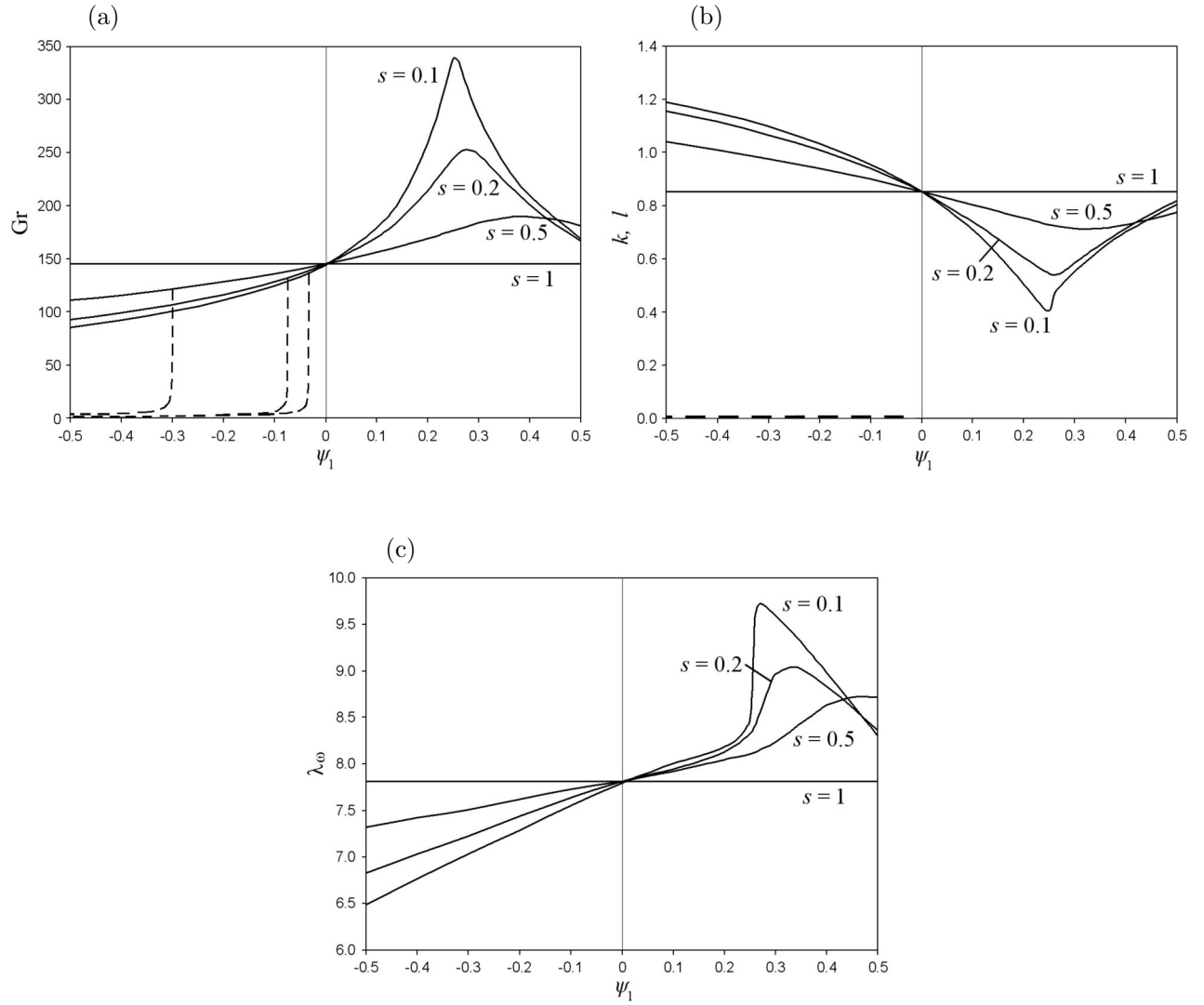


FIG. 6. The dependence of critical Grashof number (a), wave numbers (b), and frequency (c) on the separation ratio  $\psi_1$  for ternary fluid with  $\Psi=0.3$ ,  $s=Sc_{11}/Sc_{22}$ ,  $Sc_{22}=500$ . Solid and dashed lines correspond to longitudinal and transversal perturbations, respectively.

velop on the boarder line between two counterflows [Fig. 2(a)]. The perturbations of temperature and composition are localized in the central part of the slot. Note that the first component has a smaller Schmidt number (i.e., a smaller diffusion time) than the second one, so its perturbation is more diffused.

Contrary to the monotonic mode, the oscillatory mode for  $s \neq 1$  essentially depends on thermal diffusion properties of individual components. Figure 6 presents the dependence of critical Grashof number, wave numbers, and frequency on the separation ratio  $\psi_1$  at fixed  $\Psi=0.3$  for different ratios of Schmidt numbers. When the ratio of diffusion times  $s=1$ , the critical parameters coincide with those for binary mixture with  $\Psi=0.3$  (see Fig. 5) and do not change with  $\psi_1$ . With decreasing  $s$ , their variation with  $\psi_1$  becomes evident and significantly affects the stability of the system. To explain this behavior, we refer to the vertical density stratification induced by the concentration gradients of components. To calculate these gradients, we first note that the critical Grashof numbers for oscillatory instability are large enough to neglect vertical diffusion (see Sec. II E). So, the solutal

Rayleigh numbers are determined from (13), where one can safely use the approximate relation  $R/\Psi \sim 63/2$  for  $-1 < \Psi < 2$  [12]. Then from (8) and (16), we find

$$\frac{\partial \rho_1}{\partial z} = -\frac{\partial c_1}{\partial z} = -\frac{63}{2 \text{Gr} Sc_{22}} \frac{\psi_1}{s},$$

$$\frac{\partial \rho_2}{\partial z} = -\frac{\partial c_2}{\partial z} = \frac{63}{2 \text{Gr} Sc_{22}} (\psi_1 - \Psi), \quad (39)$$

$$\frac{\partial \bar{\rho}}{\partial z} = -\frac{\partial c_1}{\partial z} - \frac{\partial c_2}{\partial z} = \frac{63}{2 \text{Gr} Sc_{22}} \left( \frac{\psi_1(s-1)}{s} - \Psi \right). \quad (40)$$

The vertical density gradients are plotted in Fig. 7 for  $s=0.2$ . When  $\psi_1$  increases starting from zero, both partial density gradients are gravitationally stable ( $\partial \rho_i / \partial z < 0$ ) and the absolute value of the net density gradient  $\partial \bar{\rho} / \partial z$  is increasing. It has a stabilizing effect on the oscillatory mode (shown by solid lines in Fig. 6). At  $\psi_1=0.27$ , the stability boundary reaches maximum and then starts to decrease. Note that for

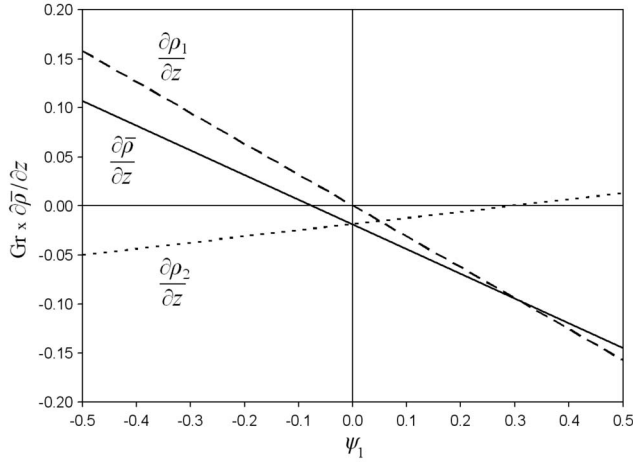


FIG. 7. The dependence of vertical density gradients on the separation ratio  $\psi_1$  for ternary fluid with  $\Psi=0.3$ ,  $s=0.2$ ,  $Sc_{22}=500$ .

$\psi_1 > 0.3$ , the partial density gradient of the second component becomes unstable. The diffusion time of this component is 5 times larger than that of the first one ( $s=0.2$ ). In this case, the fingering mechanism of double-diffusive instability [1] is evoked making the system more unstable. The change of instability mechanism is also indicated by a sharp increase of critical frequency. With increasing the difference between diffusion times of components ( $s \rightarrow 0$ ), this effect becomes even stronger. The calculations show that the oscillatory instability develops in the form of two waves with opposite phase velocities  $\lambda_\omega/k$ . A typical structure of critical pertur-

bations is presented in Fig. 9 (the perturbation corresponding to positive phase velocity is shown). Here the thermal and compositional fingers are localized near the right-hand wall, while for the perturbation with negative phase velocity (not shown) they are located near the left-hand wall. So, the critical perturbations of temperature and composition are represented by the superposition of two waves, which propagate near the lateral walls in opposite directions. Note that the fingers of the first component are more diffused than those of the second one since it has a smaller diffusion time (i.e., stronger diffusion properties). The net vertical density gradient (40) becomes gravitationally unstable for  $\psi_1 < \psi'_1$ , where

$$\psi'_1 = \frac{s\Psi}{s-1}. \quad (41)$$

The net density gradient increases when  $\psi_1$  is changing in negative direction starting from  $\psi'_1$  (for  $s=0.2$ , we have  $\psi'_1 = -0.075$ ). It has a destabilizing effect on the oscillatory mode. Note that higher critical Grashof numbers correspond to lower wave numbers  $k$  and vice versa.

For  $\psi_1 < \psi'_1$ , the transversal perturbations become more dangerous and lead to a sharp decrease of stability boundary [dashed lines on Fig. 6(a)]. This instability is associated with unstable density stratification in vertical direction. The neutral curve for transversal perturbations are presented in Fig. 10. They show that the instability is long wave but the critical Grashof number is nonzero in contrast to the binary case [see Fig. 5(a)]. The point is that for small Grashof numbers, the vertical concentration gradients depend on Gr (see Fig.

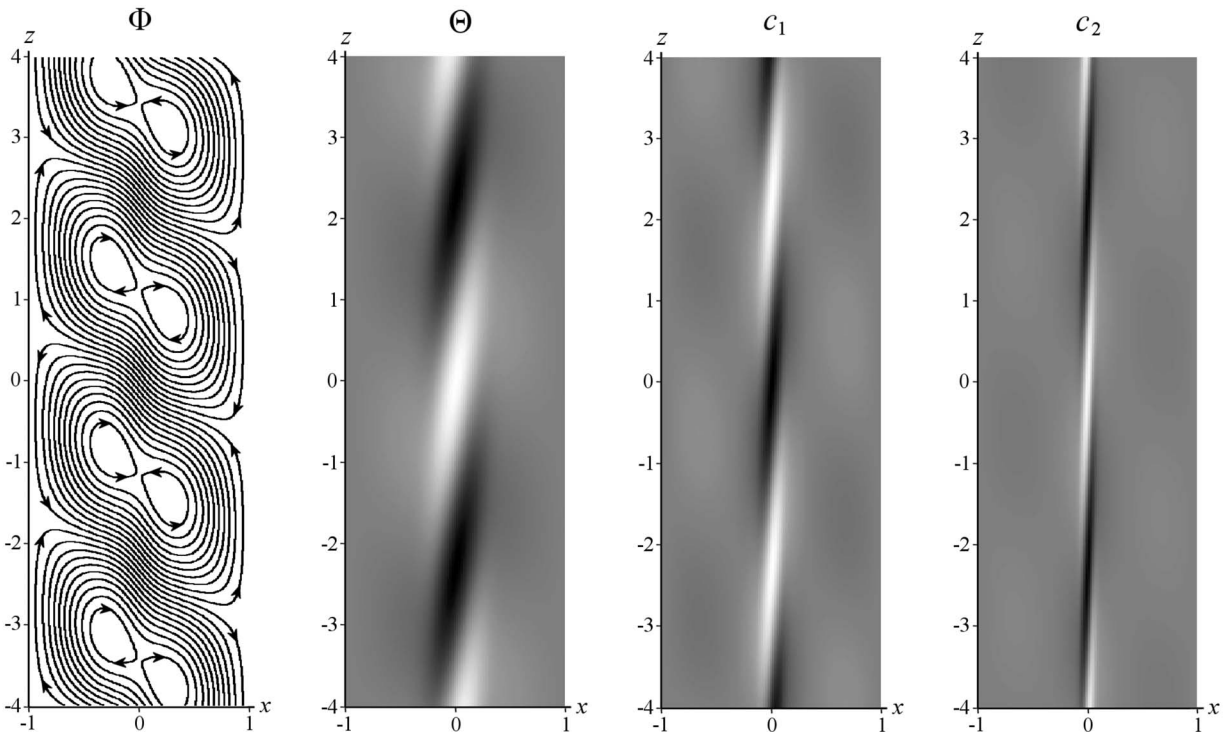


FIG. 8. Critical perturbations of velocity field, temperature, and composition for monotonic instability in ternary fluid with  $\psi_1=0.2$ ,  $\psi_2=-0.1$  ( $\Psi=0.1$ ),  $s=0.2$ ,  $Sc_{22}=500$ . The critical parameters are  $Gr=508$  and  $k=1.37$ . White and black areas correspond to positive and negative values, respectively.

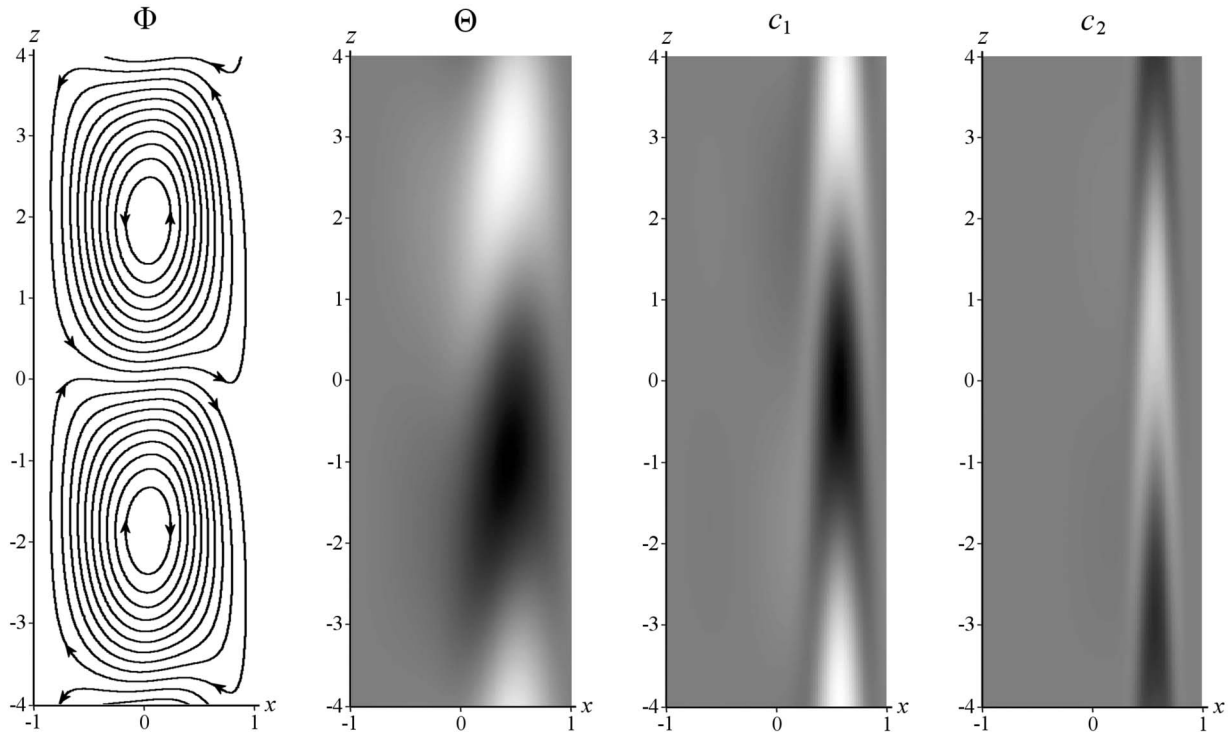


FIG. 9. Critical perturbations of velocity field, temperature, and composition for oscillatory instability in ternary fluid with  $\psi_1=0.5$ ,  $\psi_2=-0.2$  ( $\Psi=0.3$ ),  $s=0.2$ ,  $Sc_{22}=500$ . The critical parameters are  $Gr=169$ ,  $k=0.82$ ,  $\lambda_\omega=8.49$ . White and black areas correspond to positive and negative values, respectively.

3). So, the net vertical density gradient becomes unstable when  $Gr$  reaches some critical value. This value decreases when negative Soret effect of the first component becomes stronger (i.e.,  $|\psi_1|$  increases). More detailed discussion of transversal instability will be given in the next section.

**C. Ternary fluids: Transversal perturbations**

The stability of the thermogravitational column with respect to transversal perturbations is described by the problem (34)–(36). Note that the matrix of the linear system of equa-

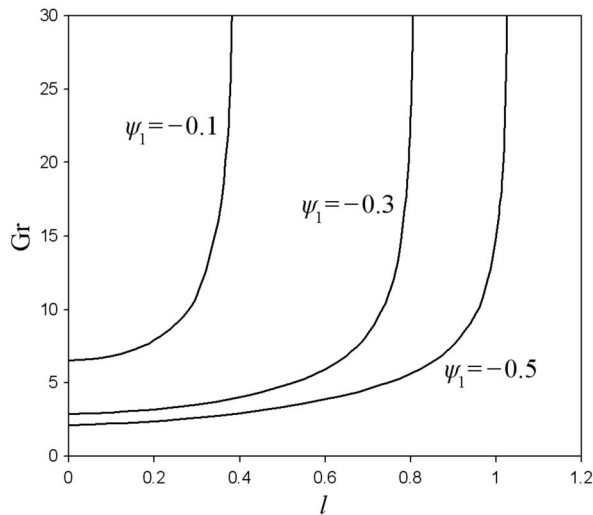


FIG. 10. Neutral curves for transversal perturbations in ternary fluid with  $\Psi=0.3$ ,  $s=0.2$ ,  $Sc_{22}=500$ .

tions for the coefficients in expansion (37) is always real, so the eigenvalues are either real or form complex-conjugate pairs. The control parameters, which determine whether the system is stable or unstable, are the solutal Rayleigh numbers  $\mathcal{R}$ . These numbers characterize the vertical gradients of composition and depend on  $S$ ,  $\psi$ , and  $Gr$ . In real TGC experiments, the spacing of the column  $L$  is chosen in such a way that vertical separation does not depend on the applied temperature difference  $\Delta T$  (i.e., the numbers  $\mathcal{R}$  do not depend on  $Gr$ , see Sec. II E). In what follows, we will consider this particular case and analyze how the physical properties of fluid ( $S$  and  $\psi$ ) affect the stability of the column. The results formulated in several statements below are valid for the general case of a multicomponent fluid. The proofs of all statements are given in the Appendix.

*Statement 3.* If solutal Rayleigh numbers  $R_i > 0$  for  $i = 1, \dots, n-1$ , then  $\mu_r > 0$ . In other words, the system is stable when the separation ratios of all components are positive (see statement 1). In this case, all partial density gradients are gravitationally stable ( $\partial\rho_i/\partial z < 0$ ).

*Statement 4.* If solutal Rayleigh numbers  $R_i < 0$  for  $i = 1, \dots, n-1$ , then  $\mu_\omega = 0$ . It means that when the separation ratios of all components are negative, the transversal perturbations are monotonic. Here all partial density gradients are gravitationally unstable ( $\partial\rho_i/\partial z > 0$ ).

These statements can be considered as analogue of exchange of stabilities principle [23] for a vertical multicomponent fluid layer with the Soret effect. The numerical calculations for binary fluid (Sec. IV A) are in agreement with these results.

*Statement 5.* If the net solutal Rayleigh number  $R > 0$  and

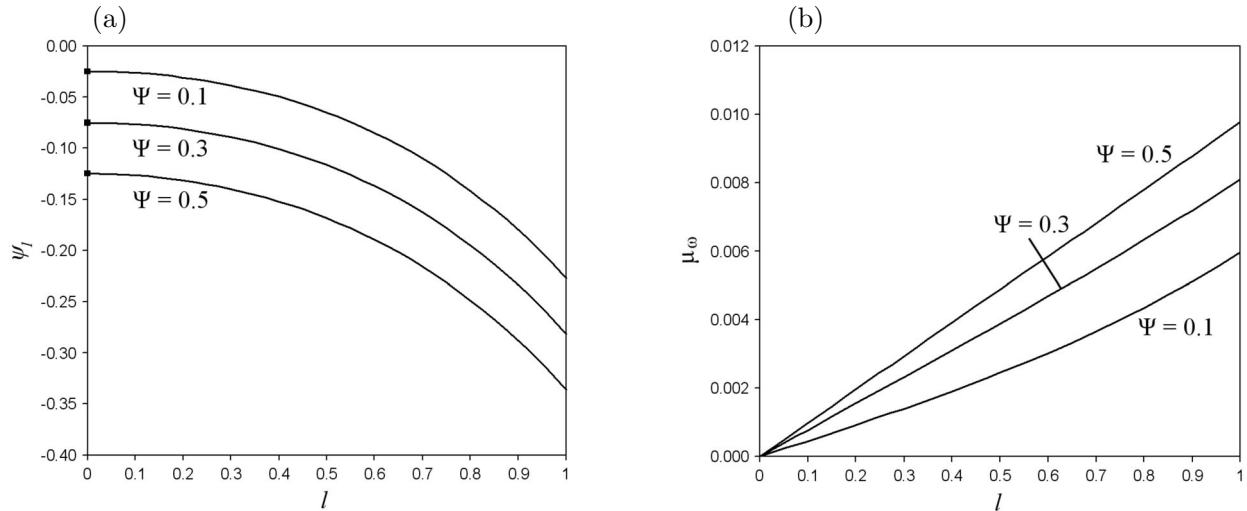


FIG. 11. The dependence of critical separation ratio  $\psi_1$  (a) and critical frequency (b) on the transversal wave number  $l$  for ternary fluid with  $s=0.2$ ,  $Sc_{22}=500$ . The system is unstable when  $\psi_1$  lies below the curves.

$\mu_r=0$ , then  $\mu_\omega \neq 0$ . The same is valid for  $R=0$  provided that the wave number  $l > 0$ . In other words, if neutral perturbations exist for  $R \geq 0$ , then they are oscillatory (except for the case  $R=l=0$ ).

It follows from statement 3 that for positive  $R$  (i.e., for positive net separation ratio  $\Psi$ ) neutral as well as unstable perturbations can exist only in ternary or higher fluids. The calculations show that they do exist in some range of control parameters, see Figs. 6 and 10. Since the solutal Rayleigh numbers are determined by the separation ratios of components [relation (13)], it is convenient to analyze the stability of the system in terms of these physical parameters. Figure 11 presents the dependence of critical separation ratio  $\psi_1$  and the critical frequency on the wave number  $l$ . The minimal absolute value of critical  $\psi_1$  is reached at  $l=0$ , so the transversal instability is long wave. We found that this critical value exactly corresponds to  $\psi'_1$  given by (41). So, the transversal instability for positive  $\Psi$  is caused by the gravitational instability of net vertical density gradient (40), which arises for  $\psi_1 < \psi'_1$ . The extensive calculations confirm this statement. In Fig. 12, the dependence of minimal critical separation ratio  $\psi_1$  on the net separation ratio  $\Psi$  is presented. The straight lines in this plot exactly correspond to those described by formula (41). With increasing  $\Psi$ , the system remains stable at larger absolute values of negative  $\psi_1$ . When the ratio of diffusion times  $s$  is decreased to zero, the unstable partial density gradient of the first component [see (39)] increases, so the system becomes less stable. According to statement 5, the onset of transversal instability for positive  $\Psi$  is oscillatory. It is clearly demonstrated by the numerical calculations [Fig. 11(b)]. Note that although the critical frequency decreases with decreasing  $l$ , it cannot be exactly zero at  $l=0$ , see statement 5.

**Statement 6.** In the range of net solutal Rayleigh numbers  $R \leq 0$ , a denumerable number of nonoscillatory neutral perturbations and corresponding critical Rayleigh numbers exist. The minimal absolute value of critical  $R$  tends to zero as  $l \rightarrow 0$ .

Numerical calculations show that for negative  $R$  (i.e., for negative net separation ratio  $\Psi$ ), the system is always un-

stable. The onset is monotonic with the critical parameters  $R=0$  and  $l=0$ . It is surprising that for negative  $\Psi$ , the system is unstable even when the net vertical density gradient is gravitationally stable. On the basis of the obtained results, we can propose the following hypothesis for the general case of a multicomponent mixture.

**Hypothesis 1.** When  $\Psi \geq 0$ , the system is stable with respect to transversal perturbations when the net vertical density gradient is gravitationally stable ( $\partial \bar{\rho} / \partial z \leq 0$ ). Otherwise, the system is unstable. The onset of instability is oscillatory with the critical wave number  $l=0$ . When  $\Psi < 0$ , the system is always unstable. The onset is monotonic with the critical wave number  $l=0$ .

For net separation ratios in the range  $-1 < \Psi < 2$ , which includes the most part of practical cases, one can safely use the approximation  $R/\Psi \sim 63/2$  in formula (13). Then the net vertical density gradient can be written as

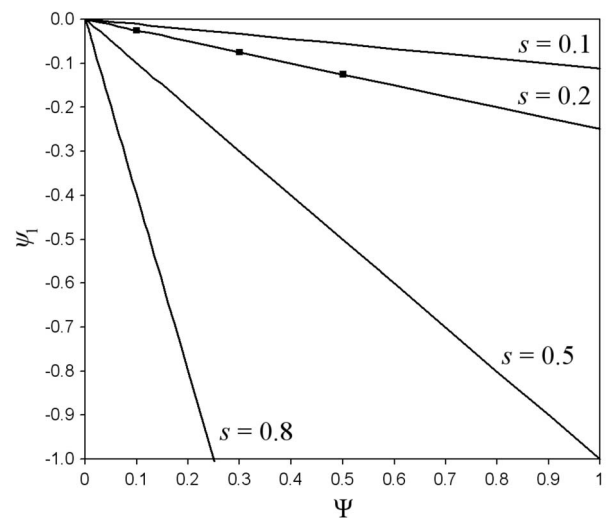


FIG. 12. The dependence of minimal critical separation ratio  $\psi_1$  on the net separation ratio  $\Psi$  for different values of  $s=Sc_{11}/Sc_{22}$  for ternary fluid with  $Sc_{22}=500$ . The three points at the line  $s=0.2$  correspond to those of Fig. 10.



$$\frac{\partial \bar{\rho}}{\partial z} = - \sum_{i=1}^{n-1} \frac{\partial c_i}{\partial z} = - \frac{63}{2 \text{Gr}} \sum_{i=1}^{n-1} \frac{\psi_i}{\text{Sc}_{ii}}. \quad (42)$$

Setting this gradient to zero, one can easily determine the stability boundary for positive  $\Psi$ . Note that the criteria expressed by hypothesis 1 are valid for mixtures with cross-diffusion effect as well since the net separation ratio and the sum of dimensionless concentrations are invariant under transformation, which eliminates cross-diffusion terms (statement 2). However, when cross-diffusion is taken into account, one should make the following replacement in (42)

$$\text{Sc}_{ii} \rightarrow \nu_i^{-1}, \quad \psi \rightarrow P^{-1} Q \psi,$$

where  $\nu_i$  are the eigenvalues of the matrix  $\mathcal{S}$  (see also Sec. III C).

The obtained results indicate that a plane thermogravitational column can be used for measuring the transport coefficients in ternary and higher mixtures when one or several components have negative Soret effect. In binary systems, such measurements are possible for positive Soret effect only. It should be noted that in real columns, the transversal instability sets in at the maximal possible wavelength, which is equal to the transversal width of the column. It follows from Fig. 11(a) that the decrease of this width has a stabilizing effect on the transversal mode.

## V. CONCLUSION

In this work, we have first performed a comprehensive linear stability analysis of convection in a plane thermogravitational column with a multicomponent fluid. A particular attention is focused on binary and ternary mixtures. The basic state describing the steady flow and separation in a multicomponent fluid is derived. An effective formalism is used to describe thermal diffusion and convection in mixtures with many components. The stability with respect to two types of perturbations is investigated: Longitudinal waves (in the plane of vertical axis and temperature gradient) and transversal waves (in the plane perpendicular to the temperature gradient). The stability problems are reduced to those without cross-diffusion effect by a special transformation and then solved by the Galerkin method.

The calculations show that in binary fluids with positive separation ratio  $\Psi$ , the onset of longitudinal instability is oscillatory. The decrease of Schmidt number has a stabilizing effect on the oscillatory mode. The monotonic mode becomes more dangerous when  $\Psi$  decreases approaching to zero. For negative  $\Psi$ , the system is always unstable with respect to long-wave transversal perturbations due to destabilizing vertical stratification. The stability map for binary fluids is valid in ternary case provided that the two principle components have the same diffusive properties. Otherwise, the Soret effect can stabilize or destabilize the oscillatory mode depending on the separation ratios of components  $\psi_1$  and  $\psi_2$ . The transversal instability in ternary fluids essentially depends on the net separation ratio  $\Psi = \psi_1 + \psi_2$ . For  $\Psi \geq 0$ , the system is stable (unstable) when the vertical density gradient is stabilizing (destabilizing). Surprisingly, the

system is always unstable for  $\Psi < 0$  regardless of vertical density stratification. The onset of long-wave transversal instability is oscillatory for  $\Psi \geq 0$  and monotonic for  $\Psi < 0$ . It is argued that these results are valid in the general case of a multicomponent fluid. The analogue of exchange of stabilities principle for a plane column with a multicomponent fluid is proved: The system is stable with respect to transversal perturbations when all components have positive Soret effect ( $\psi_i > 0$ ); when all of them have negative Soret effect ( $\psi_i < 0$ ), the growth of perturbations is monotonic. It should be noted that strong destabilization of the column for fluids with negative Soret effect cannot be revealed by considering two-dimensional perturbations in the plane of vertical axis and temperature gradient.

The obtained results are presented in the form, which is rather simple and convenient for specialists in experimental measurements. We conclude that a plane thermogravitational column can be used for measuring the transport coefficients in ternary and higher mixtures when one or several components have negative Soret effect. In binary systems, such measurements are possible for positive Soret effect only. The decrease of transversal column width has a stabilizing effect on transversal instability and allows one to perform measurements in fluids with larger negative Soret effect.

## ACKNOWLEDGMENT

This work is supported by the PRODEX programme of the Belgian Federal Science Policy Office.

## APPENDIX

*Proof of statements 3 and 4.* Consider problem (34)–(36) assuming that the matrix  $\mathcal{S}$  is diagonal,

$$w'' - l^2 w + \mathbf{I} \cdot \boldsymbol{\xi} = -\mu w, \quad (\text{A1})$$

$$\text{Sc}_{ii}^{-1} (\xi_i'' - l^2 \xi_i - R_i w) = -\mu \xi_i, \quad (\text{A2})$$

$$x = \pm 1, \quad w = 0, \quad \xi_i' = 0, \quad (\text{A3})$$

where  $i=1, \dots, n-1$ . Let us multiply equations (A1) and (A2) by  $\bar{w}$  and  $\bar{\xi}_i$ , respectively (the bar denotes a complex-conjugate value). Integrating the resulting equations from  $-1$  to  $1$  taking into account boundary conditions (A3), we find

$$\int (w')^2 dx + l^2 \int w^2 dx - \int \mathbf{I} \cdot \boldsymbol{\xi} \bar{w} dx = \mu \int w^2 dx, \quad (\text{A4})$$

$$\text{Sc}_{ii}^{-1} \left( \int (\xi_i')^2 dx + l^2 \int \xi_i^2 dx + R_i \int w \bar{\xi}_i dx \right) = \mu \int \xi_i^2 dx. \quad (\text{A5})$$

Here and below the limits of integration are omitted for brevity. Let us sum up Eq. (A4) and its complex conjugate. Similarly, Eq. (A5) is multiplied by  $\text{Sc}_{ii}/R_i$  and added to its complex conjugate. Summing up the resulting equations over  $i=1, \dots, n-1$ , we obtain



$$(\bar{\mu} + \mu) \int w^2 dx = 2 \int (w')^2 dx + 2l^2 \int w^2 dx - \int (\mathbf{I} \cdot \xi \bar{w} + \mathbf{I} \cdot \bar{\xi} w) dx, \quad (\text{A6})$$

$$(\bar{\mu} + \mu) \sum_{i=1}^{n-1} \frac{\text{Sc}_{ii}}{R_i} \int \xi_i^2 dx = \sum_{i=1}^{n-1} \frac{2}{R_i} \left( \int (\xi_i')^2 dx + l^2 \int \xi_i^2 dx \right) + \int (\mathbf{I} \cdot \xi \bar{w} + \mathbf{I} \cdot \bar{\xi} w) dx. \quad (\text{A7})$$

The sum of (A6) and (A7) is given by

$$(\bar{\mu} + \mu) \left( \int w^2 dx + \sum_{i=1}^{n-1} \frac{\text{Sc}_{ii}}{R_i} \int \xi_i^2 dx \right) = 2 \int (w')^2 dx + 2l^2 \int w^2 dx + \sum_{i=1}^{n-1} \frac{2}{R_i} \left( \int (\xi_i')^2 dx + l^2 \int \xi_i^2 dx \right).$$

All integrals in this relation are positive. When  $R_i > 0$  for  $i = 1, \dots, n-1$ , we have  $\bar{\mu} + \mu > 0$ . It follows that  $\mu_r > 0$ , which proves statement 2.

Let us now subtract Eq. (A4) from its complex conjugate. Similarly, Eq. (A5) is multiplied by  $\text{Sc}_{ii}/R_i$  and subtracted from its complex conjugate. Summing up the resulting equations over  $i = 1, \dots, n-1$ , we obtain

$$(\bar{\mu} - \mu) \int w^2 dx = \int (\mathbf{I} \cdot \xi \bar{w} - \mathbf{I} \cdot \bar{\xi} w) dx, \quad (\text{A8})$$

$$(\bar{\mu} - \mu) \sum_{i=1}^{n-1} \frac{\text{Sc}_{ii}}{R_i} \int \xi_i^2 dx = \int (\mathbf{I} \cdot \xi \bar{w} - \mathbf{I} \cdot \bar{\xi} w) dx. \quad (\text{A9})$$

Subtracting (A9) from (A8) gives

$$(\bar{\mu} - \mu) \left( \int w^2 dx - \sum_{i=1}^{n-1} \frac{\text{Sc}_{ii}}{R_i} \int \xi_i^2 dx \right) = 0.$$

When  $R_i < 0$  for  $i = 1, \dots, n-1$ , the second multiplier is always positive, so  $\bar{\mu} - \mu = 0$ . It follows that  $\mu_\omega = 0$ , which proves statement 3.

*Proof of statement 5.* Suppose that conditions of the statement are satisfied and  $\mu_\omega = 0$ . The eigenfunctions, which correspond to the eigenvalue  $\mu = 0$  satisfy the problem

$$w'' - l^2 w + \mathbf{I} \cdot \xi = 0, \quad (\text{A10})$$

$$\xi'' - l^2 \xi - \mathcal{R} w = 0, \quad (\text{A11})$$

$$x = \pm 1, \quad w = 0, \quad \xi' = 0. \quad (\text{A12})$$

Let us differentiate Eq. (A10) two times and substitute the expression for  $\xi''$  from (A11) into the resulting equation. Expressing  $\mathbf{I} \cdot \xi$  in terms of  $w$  from (A10) and taking into account the boundary conditions, we find

$$w'''' - 2l^2 w'' + (l^4 + R)w = 0, \quad (\text{A13})$$

$$x = \pm 1, \quad w = 0, \quad w''' - l^2 w' = 0. \quad (\text{A14})$$

Note that real and imaginary parts of functions  $w$  and  $\xi$  satisfy the same problem, so only real solutions can be considered. The general solution of Eq. (A13) for  $R > 0$  is given by [26]

$$w = e^{-\alpha x} (a_1 \cos \beta x + a_2 \sin \beta x) + e^{\alpha x} (a_3 \cos \beta x + a_4 \sin \beta x),$$

$$\alpha = \sqrt{\frac{\sqrt{l^4 + R} + l^2}{2}}, \quad \beta = \sqrt{\frac{R}{2\sqrt{l^4 + R} + 2l^2}},$$

while for  $R = 0$  and  $l > 0$  it is written as

$$w = e^{-lx} (a_1 + a_2 x) + e^{lx} (a_3 + a_4 x).$$

Here  $a_1 - a_4$  are real constants to be determined from boundary conditions (A14). It can be checked that the determinant of the corresponding linear system of equations is nonzero. It follows that all constant are zero, so  $w = 0$ . Then from (A11) and (A12) we find  $\xi = 0$ . It follows that  $\mu = 0$  is not an eigenvalue of problem (34)–(36). This contradiction proves the statement. As for the case  $R = l = 0$ , it is easy to show that in this case there exist nonoscillatory neutral perturbations of the form  $w = 0$ ,  $\xi = \text{const}$ .

*Proof of statement 6.* The neutral nonoscillatory perturbations of velocity satisfy problem (A13) and (A14). It was shown in [24] that for  $R < 0$  this problem has a denumerable number of eigenvalues  $R$  (i.e., critical net solutal Rayleigh numbers) and corresponding eigenfunctions. The minimal critical number  $|R| \rightarrow 0$  as  $l \rightarrow 0$ .

[1] J. S. Turner, *Annu. Rev. Fluid Mech.* **17**, 11 (1985).

[2] J. K. Platten, *J. Appl. Mech.* **73**, 5 (2006).

[3] S. Wiegand, *J. Phys.: Condens. Matter* **16**, R357 (2004).

[4] A. Mialdun and V. Shevtsova, *Int. J. Heat Mass Transfer* **51**, 3164 (2008).

[5] K. Clusius and G. Dickel, *Naturwiss.* **26**, 546 (1938).

[6] W. H. Furry, R. C. Jones, and L. Onsager, *Phys. Rev.* **55**, 1083 (1939).

[7] B. I. Nikolaev and A. A. Tubin, *J. Eng. Phys.* **18** (5), 540

(1970).

[8] J. L. Navarro, J. A. Madariaga, and J. M. Savirón, *J. Phys. A* **15**, 1683 (1982).

[9] G. Labrosse, *Phys. Fluids* **15**, 2694 (2003).

[10] K. Haugen and A. Firoozabadi, *J. Chem. Phys.* **122**, 014516 (2005).

[11] K. Haugen and A. Firoozabadi, *J. Chem. Phys.* **127**, 154507 (2007).

[12] I. I. Ryzhkov and V. M. Shevtsova, *Phys. Fluids* **19**, 027101

- (2007).
- [13] M. M. Bou-Ali and J. K. Platten, *J. Non-Equil. Thermodyn.* **30**, 385 (2005).
- [14] A. Leahy-Dios, M. M. Bou-Ali, J. K. Platten, and A. Firoozabadi, *J. Chem. Phys.* **122**, 234502 (2005).
- [15] L. Onsager and W. W. Watson, *Phys. Rev.* **56**, 474 (1939).
- [16] B. Nikolaev and A. Tubin, *J. Appl. Math. Mech.* **35**, 214 (1971).
- [17] A. Zebib, *J. Non-Equil. Thermodyn.* **32**, 211 (2007).
- [18] I. I. Ryzhkov and V. M. Shevtsova, *Phys. Fluids* **21**, 014102 (2009).
- [19] M. M. Bou-Ali, O. Ecenarro, J. A. Madariaga, and C. M. Santamaría, *Phys. Rev. E* **59**, 1250 (1999).
- [20] O. Batiste, A. Alonso, and I. Mercader, *J. Non-Equil. Thermodyn.* **29**, 359 (2004).
- [21] R. Kita, S. Wiegand, and J. Luettmmer-Strathmann, *J. Chem. Phys.* **121**, 3874 (2004).
- [22] J. K. Platten, M. M. Bou-Ali, and J. F. Dutrieux, *J. Phys. Chem. B* **107**, 11763 (2003).
- [23] P. G. Drazin and W. H. Reid, *Hydrodynamic Stability* (Cambridge University Press, Cambridge, 1981).
- [24] G. Z. Gershuni and E. M. Zhukhovitskii, *Convective Stability of Incompressible Fluids* (Keter Press, Jerusalem, 1976).
- [25] I. Ryzhkov and V. Shevtsova, *Microgravity Sci. Technol.* **21**, 37 (2009).
- [26] A. D. Polyanin and V. F. Zaitsev, *Handbook of Exact Solutions for Ordinary Differential Equations* (CRC Press, Boca Raton, FL, 2002).